Mechanics of Materials 134 (2019) 106–114

Contents lists available at ScienceDirect

Mechanics of Materials

journal homepage: www.elsevier.com/locate/mechmat

Diffusion-driven stress relaxation of gels under incremental planar extensions

Raffaella De Vita[a], Paola Nardinocchi[*,b], Luciano Teresi[c]

[a] STRETCH Laboratory, Department of Biomedical Engineering and Mechanics, Virginia Tech, Blacksburg, VA 24061, USA
[b] Dipartimento di Ingegneria Strutturale e Geotecnica Sapienza Università di Roma, Roma I-00184, Italy
[c] Dipartimento di Matematica e Fisica Università Roma Tre, Roma I-00184, Italy

ARTICLE INFO

Keywords:
Diffusion
Stress relaxation
Planar extension
Incremental extension
Hydrogels

ABSTRACT

We investigated the stress response of hydrogels to multiple and consecutive planar extensions using the standard Flory–Rehner thermodynamics. We show explicitly how the stress relaxation at a given extension depends on both the number and magnitude of incremental steps that lead to such extension. These results have the potential to impact the design of hydrogel-based actuators where a prescribed extension can be achieved through several consecutive extensions.

1. Introduction

Hydrogels are soft materials made of cross–linked networks of hydrophilic polymers that swell in water. The degree of swelling depends on the amount of water uptake; for a given gel, the water uptake is determined by the chemical potential of the environment and by the applied loads. It is well known that hydrogels swell more when they are under tension than when they are in a stress-free state or are under compression. Moreover, under tension at a constant strain, the stress within the gel decreases significantly due to the water uptake that creates an increase in the gel volume as described elsewhere (Takigawa et al., 1993; Urayama et al., 1994; Hong et al., 2009; Yohsuke et al., 2011; Urayama and Takigawa, 2012; Fujine et al., 2015). In the above cited experimental studies, the hydrogel is stretched and the stress relaxation is computed as the difference between the instantaneous stress, that is the stress of a gel treated as an incompressible elastic solid before diffusion starts, and the steady stress, that is the stress when the balance between the chemical potentials of the solvent inside and outside the gel is achieved. In particular, in Fujine et al. (2015) biaxial tests from a pre-stretched configuration are also discussed.

Throughout this manuscript, the instantaneous stress response at time scales prior to diffusion and the long term stress response at time scales where diffusion has completed its action will be termed the *fast stress* and *slow stress*, respectively. This fast and slow response regimes are similar to those observed in viscoelastic materials even though the stress relaxation mechanism in these materials is typically different (Wineman and Rajagopal, 1992).

Strain-driven swelling and stress reduction under uniaxial and biaxial stretching are investigated thoroughly for isotropic gels in Takigawa et al. (1993), Urayama et al. (1994), Yohsuke et al. (2011), Urayama and Takigawa (2012) and Fujine et al. (2015), whereas the fast and slow stress responses of anisotropic gels under uniaxial stretching are studied in Nardinocchi et al. (2015a) and Nardinocchi and Teresi (2016). The stress relaxation and change in volume of the gels have been shown to depend on the type of biaxial deformation (Fujine et al., 2015). However, while there are recent studies on the coupling between biaxial deformations and swelling (Pence, 0000; Selvadurai and Suvorov, 2017) there are currently no studies on the effect of multiple and consecutive planar extensions on the mechanical behavior of gels despite the relevance of such deformations in real applications for gels as soft actuators.

In this manuscript, we analyze the stress response of gels under incremental extensions within the context of the standard Flory–Rehner thermodynamics modeling framework. Precisely, we consider three types of deformations: planar, equibiaxial, and unequal biaxial extensions. We define the incremental extension as a series of extensions and, at each extension increment, we compute the fast stress response of the hydrogel and then we evaluate the subsequent stress reduction due to the diffusion.

The manuscript is structured as follows. In Section 2, we briefly present the main characteristics of the stress-diffusion modeling framework. In Section 3, we introduce the specific equations that describe the response of gels to incremental extensions. Moreover, we explicitly evaluate the stress reduction due to a single extension and the stress

* Corresponding author.
E-mail addresses: devita@vt.edu (R.D. Vita), paola.nardinocchi@uniroma1.it (P. Nardinocchi), teresi@uniroma3.it (L. Teresi).

https://doi.org/10.1016/j.mechmat.2019.04.016
Received 4 February 2019; Received in revised form 24 April 2019; Accepted 24 April 2019
Available online 25 April 2019

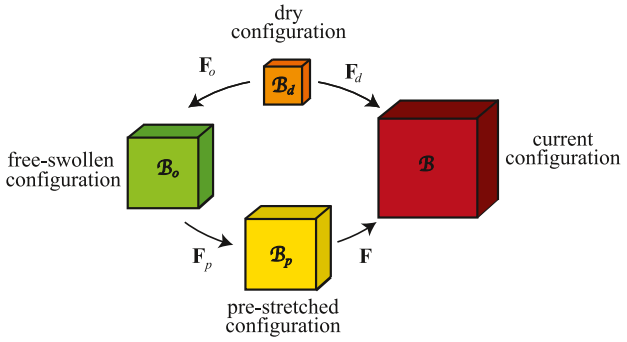

Fig. 1. Sketch of the deformation maps relating the dry state, $\mathcal{B}_d$, the stress–free swollen state, $\mathcal{B}_o$, the pre-stretched state, $\mathcal{B}_p$, and the current state, $\mathcal{B}$.

reduction due to two consecutive extensions that lead to the same total elongation. In Section 4, we consider different types of planar extesions and discuss the corresponding responses in terms of stresses and changes in volume.

2. Background

We consider the multiphysics modeling framework discussed in Lucantonio et al. (2013). In Lucantonio et al. (2013), the balance equations and constitutive equations were presented in detail and the evolution equations governing swelling and de–swelling in gels were derived. We find useful to re-introduce here some key states of a body made of gel: a dry state, $\mathcal{B}_d$, with a volume V_d, a stress–free swollen state, $\mathcal{B}_o$, with a volume V_o, a pre-stretched state, $\mathcal{B}_p$, with volume V_p, and an actual steady state, $\mathcal{B}$, with volume V determined by mechanical and chemical stimuli (Fig. 1).

The process that leads one body to change state may be complex and can be studied by using numerical methods (Bertrand et al., 2016; Curatolo et al., 2017). However, the stress–free state $\mathcal{B}_o$ as well as the pre-stretched state $\mathcal{B}_p$ can be easily determined from the hydration and deformation states. Likewise, under certain loads and constraints, the actual steady state $\mathcal{B}$ can easily characterized when it is attained from $\mathcal{B}_p$ through a homogenous field of deformation (which implies a homogeneous state of hydration). In these cases, chemical and mechanical boundary conditions completely determine the actual state of the gel, once the constitutive equations are selected (Nardinocchi and Teresi, 2016).

2.1. Constitutive theory

The constitutive equations for the stress $\mathbf{S}_d$ ($[\mathbf{S}_d]=\text{Pa}=\text{J/m}^3$) relative to the dry configuration $\mathcal{B}_d$ and for the chemical potential μ ($[\mu]=\text{J/mol}$) are derived from the theoretical framework proposed and discussed in Nardinocchi et al. (2015a, 2015b) and Nardinocchi and Teresi (2016), based on the Flory–Rehner thermodynamic model.

The free energy per unit dry volume, ψ, is assumed to be the sum of an elastic free energy ψ_e, and a polymer–solvent mixing free energy ψ_m. The former depends on the deformation gradient $\mathbf{F}_d$ that defines the deformation from the initial dry configuration of the gel (Fig. 1) and the latter depends on the molar solvent concentration c_d per unit dry volume ($[c_d]=\text{mol/m}^3$). It is assumed that changes in volume are only due to solvent absorption or release. Then, the free energy ψ can be as follows:

$$\psi(\mathbf{F}_d, c_d, p) = \psi_e(\mathbf{F}_d) + \psi_m(c_d) - p(J_d - \hat{J}(c_d)). \tag{2.1}$$

where p serves to enforce the volumetric constraint according to which the volume change due to the deformation, $J_d = \det \mathbf{F}_d$, is equal to the volume change due to solvent absorption or release, $\hat{J}(c_d) = 1 + \Omega c_d$. This requires that

$$\det \mathbf{F}_d = 1 + \Omega c_d, \tag{2.2}$$

where Ω ($[\Omega]=\text{m}^3/\text{mol}$) is the solvent molar volume. The nominal stress $\mathbf{S}_d$ and the chemical potential μ are derived from thermodynamics principles:

$$\mathbf{S}_d = \hat{\mathbf{S}}_d(\mathbf{F}_d) - p(\det \mathbf{F}_d)\mathbf{F}_d^{-T} \quad \text{with} \quad \hat{\mathbf{S}}_d(\mathbf{F}_d) = \frac{\partial \psi_e}{\partial \mathbf{F}_d} \tag{2.3}$$

and

$$\mu = \hat{\mu}(c_d) + p\Omega \quad \text{with} \quad \hat{\mu}(c_d) = \frac{\partial \psi_m}{\partial c_d}. \tag{2.4}$$

As standard in Flory–Rehner theory, we assume that the gel is isotropic and undergoes large deformations so that it can be described by the following elastic free energy:

$$\psi_e(\mathbf{F}_d) = \frac{G}{2}(\mathbf{C}_d \cdot \mathbf{I} - 3), \tag{2.5}$$

where G ($[G]=\text{J/m}^3$) is the shear modulus of the dry polymer and $\mathbf{C}_d = \mathbf{F}_d^T\mathbf{F}_d$. From $(2.3)_2$ and (2.5), we can easily compute the stress $\hat{\mathbf{S}}_d(\mathbf{F}_d)$ relative to the dry configuration and then compute the corresponding Cauchy stress $\mathbf{T}$ as

$$\mathbf{T} = \hat{\mathbf{T}}(\mathbf{F}_d) - p\mathbf{I}, \quad \hat{\mathbf{T}}(\mathbf{F}_d) = \frac{1}{J_d}\hat{\mathbf{S}}_d(\mathbf{F}_d)\mathbf{F}_d^T. \tag{2.6}$$

Following Flory and Rehner (1943a,b), we also prescribe the following polymer–solvent mixing energy:

$$\psi_m(c_d) = \frac{RT}{\Omega} h(c_d), \tag{2.7}$$

with

$$h(c_d) = \Omega c_d \log\frac{\Omega c_d}{1 + \Omega c_d} + \chi \frac{\Omega c_d}{1 + \Omega c_d}, \quad [h] = 1, \tag{2.8}$$

where R ($[R]=\text{J/(K mol)}$), T ($[T]=\text{K}$), and χ are the universal gas constant, the temperature, and the Flory parameter, respectively. From $(2.4)_2$, (2.7), and (2.8) we can easily find the chemical potential $\hat{\mu}(c_d)$. By exploiting the volumetric constraint (2.2), the chemical potential can be rewritten as function of J_d with a slight abuse of notation:

$$\hat{\mu}(c_d) = \hat{\mu}(J_d) = RT\left(\log\frac{J_d - 1}{J_d} + \frac{1}{J_d} + \frac{\chi}{J_d^2}\right). \tag{2.9}$$

The material parameters are assumed to have values that are typical for soft hydrogels:

$$\Omega = 1.8\cdot10^{-5}\,\text{m}^3/\text{mol},\ R = 8.314\,\text{J/(K mol)},\ T = 293\,\text{K},\ \chi = 0.5,\ G = 10^5\,\text{Pa}. \tag{2.10}$$

2.2. Stress-free swollen state

Given the dry state $\mathcal{B}_d$ of a gel, the stress–free swollen state $\mathcal{B}_o$ is completely defined by the value of the chemical potential μ_e of the solvent in which the gel is immersed through the mechanical and chemical balance laws: $\mathbf{S}_d = \mathbf{0}$ and $\mu = \mu_e$. More precisely, the stress-free swollen state can be described by the homogeneous deformation field $\mathbf{F}_o = \lambda_o\mathbf{I}$, where λ_o is the stretch ratio. Hence, from the Eqs. (2.3) and (2.5), the stress $\mathbf{S}_d$ that corresponds to $\mathbf{F}_d = \mathbf{F}_o$ is $\mathbf{S}_d = (G\lambda_o - p\lambda_o^2)\mathbf{I}$, and the stress-free condition implies that $p = G/\lambda_o$. Substituting p in the relation for the chemical potential (2.4) yields a nonlinear equation relating μ_e and λ_o:

$$\hat{\mu}(J_o) + \frac{G}{\lambda_o}\Omega = \mu_e, \quad \text{with} \quad J_o = \lambda_o^3. \tag{2.11}$$

The volume of the swollen gel is then $V_o = J_o V_d$; the values (2.10) yields $J_o \simeq 10.2$. If we assume that the gel in our dry state $\mathcal{B}_d$ is a parallelepiped with sides L_d, L_d, and h_d, the gel in the stress-free swollen state $\mathcal{B}_o$

is still a parallelepiped but has sides $L_o = \lambda_o L_d$, $L_o = \lambda_o L_d$, and $h_o = \lambda_o\, h_d$. For large deformation ($1/J_o \to 0$), Eq. (2.9) can be approximated to

$$\hat{\mu}(J_o) \simeq RT(\chi - 1/2)\frac{1}{J_o^2}\,, \tag{2.12}$$

so that Eq. (2.11) can be written as

$$\frac{RT}{\Omega}(\chi - 1/2) = \left(\frac{\mu_e}{\Omega} - \frac{G}{\lambda_o}\right)J_o^2\,. \tag{2.13}$$

Eq. (2.13) provides an explicit estimate of the quantity $RT(\chi - 1/2)$ in terms of the chemical potential μ_e of the solvent in which the gel is immersed and the stretch λ_o due to stress-free swelling.

2.3. Pre-stretched state

We introduce a pre-stretched configuration of the gel since such configuration is usually the configuration from which the elastic stress-stretch and stress relaxation data of gels are collected via mechanical tests (Fujine et al., 2015). The introduction of this configuration is necessary for determining the stress response due to unequal planar extensions as discussed in Section 3. The pre-stretched configuration $\mathcal{B}_p$ of the gel differs from the stress-free configuration $\mathcal{B}_o$ and is described by the deformation gradient $\mathbf{F}_d = \mathbf{F}_p\,\mathbf{F}_o$ as shown in Fig. 1.

We consider a parallelepiped-shaped gel of side lengths L_o, L_o, and h_o. The three sides of this parallelepiped are aligned with the unit vectors of the standard basis $\mathbf{e}_1$, $\mathbf{e}_2$, and $\mathbf{e}_3$ in the $\mathcal{B}_p$ configuration and the gel is extended in the plane defined by $\mathbf{e}_1$ and $\mathbf{e}_2$. We assume that the gel is deformed from the stress-free swollen state $\mathcal{B}_o$ by applying a stretch $\lambda_{p\alpha}$ ($\alpha = 1, 2$) along $\mathbf{e}_\alpha$ so, in the pre-stretched state, the lengths of two sides of the parallelepiped are

$$L_{p\alpha} = \lambda_{p\alpha} L_o\,. \tag{2.14}$$

The thickness h_p in the pre-stretched state is determined by the balance of forces and solvent concentration through the boundary conditions on the stress and the chemical potential, that is: $\sigma_3 = \mathbf{Te}_3\cdot\mathbf{e}_3 = 0$ and $\mu = \mu_e$. For example, for isotropic gels, Eqs. (2.3), (2.5), and (2.6), lead to

$$\sigma_3 = \frac{G}{J_d}\lambda_{d3}^2 - p \quad \text{with} \quad J_d = J_p\, J_o \quad \text{and} \quad J_p = \lambda_{p1}\lambda_{p2}\lambda_{p3} \tag{2.15}$$

and $\lambda_{d3} = \lambda_{p3}\lambda_o$. Therefore, since $\sigma_3 = 0$, it follows

$$p = \frac{G}{J_d}\lambda_{d3}^2\,. \tag{2.16}$$

Substituting this value of p into Eqs. (2.4), from the chemical balance law it follows that

$$\hat{\mu}(J_d) + \Omega\frac{G}{J_d}\lambda_{d3}^2 = \mu_e\,. \tag{2.17}$$

The above equation provides the value of λ_{p3} when the balance of the chemical potentials of the solvent inside and outside the gel is achieved. Consequently, the thickness h_p of the gel can be computed as $h_p = \lambda_{p3}h_o$.

The (plane) stress of the gel in the $\mathcal{B}_p$ configuration is described by the only non-zero axial components of the Cauchy stress $\mathbf{T}$:

$$\sigma_\alpha = \frac{G}{J_d}\lambda_{d\alpha}^2 - p\,, \quad \text{with} \quad \lambda_{d\alpha} = \lambda_{p\alpha}\lambda_o\,, \tag{2.18}$$

which can be rewritten using Eq. (2.16) as

$$\sigma_1 = \frac{G}{\lambda_o}\left(\frac{\lambda_{p1}}{\lambda_{p2}\lambda_{p3}} - \frac{\lambda_{p3}}{\lambda_{p1}\lambda_{p2}}\right),$$
$$\sigma_2 = \frac{G}{\lambda_o}\left(\frac{\lambda_{p2}}{\lambda_{p1}\lambda_{p3}} - \frac{\lambda_{p3}}{\lambda_{p1}\lambda_{p2}}\right). \tag{2.19}$$

We explicitly note that when $\lambda_{p\alpha} = 1$, Eq. (2.15) gives $\lambda_{p3} = 1$ and Eqs. (2.19) lead to $\sigma_{p\alpha} = 0$. This means that the $\mathcal{B}_p$ and $\mathcal{B}_o$ configurations are identical.

In the following section, we will consider the stress response of gels subjected to different types of planar extensions. Since our goal is comparing, at least qualitatively, the model with experimental data, we will assume that stress data on gels are recorded starting from a pre-stretched state for unequal biaxial extensions.

3. Isotropic gels under incremental biaxial extensions

During stress relaxation tests as those described in Urayama and Takigawa (2012) and Fujine et al. (2015), gels are first stretched up to a fixed stretch quickly before diffusion starts. The elastic stress at this fixed stretch, which is here called the *fast stress*, is measured. Then, the gel is kept under this constant stretch over a long time interval that allows diffusion to occur. The stress after diffusion occurs, which is here termed the *slow stress*, is measured. The difference between fast and slow stresses is known as *stress relaxation* and this relaxation is assumed to be determined solely by swelling. In Fujine et al. (2015), the agreement between the standard Flory–Rehner thermodynamic model and biaxial experimental data was discussed in details (see also references therein). Here, we aim to determine both the fast and the slow stresses for isotropic gels subjected to incremental planar extensions. In particular, after denoting with L_α the side lengths of a parallelepiped-shaped gel along the unit vector $\mathbf{e}_\alpha$, we consider three different biaxial extensions:

1. A planar extension where the side length L_1 is increased while $L_2 = 1$ is fixed;
2. An equibiaxial extension where the side lengths L_1 and L_2 are increased by the same amount.
3. An unequal biaxial extension where the side lengths are increased so that $L_2 = (3/2)\,L_1$.

3.1. Incremental planar and equibiaxial extensions

We assume that the parallelepiped-shaped gel introduced in Section (2.3) is subjected to incremental planar or equibiaxial extensions from the swollen configuration $\mathcal{B}_o$. More precisely, for N consecutive times, the gel is stretched only in the direction $\mathbf{e}_1$ by $\Delta\lambda_1$ or in the two perpendicular directions $\mathbf{e}_1$ and $\mathbf{e}_2$ by equal amounts $\Delta\lambda_1 = \Delta\lambda_2$. The gel is then allowed to relax due to diffusion. Let $L_1^{\max}$ be the maximal side length of the gel that is achieved at the Nth extension. We assume that for an equi-biaxial extension $L_1^{\max} = L_2^{\max}$.

At the kth extension, the side length of the gel increases from its initial value $L_1^{(k-1)}$ to its final value $L_1^{(k)}$ ($k = 1, \cdots, N$), where $L_1^{(0)} = L_o$. After introducing $\Delta\lambda_1$ as

$$\Delta\lambda_1 = \frac{1}{N}\left(\frac{L_1^{\max} - L_o}{L_o}\right), \tag{3.20}$$

we define the constant incremental stretch, $\bar{\lambda}_1^{(k)}$, at the kth stress relaxation as

$$\bar{\lambda}_1^{(k)} = \frac{1 + k\Delta\lambda_1}{1 + (k-1)\Delta\lambda_1}\,. \tag{3.21}$$

Let us consider the case in which the side lengths and thickness of the gel are L_o, L_o, and h_o in the swollen configuration $\mathcal{B}_o$. Without loss of generality, we can assume that the maximal side length that is attained by the gel in N steps is $L_1^{\max} = 3L_o$. Then, for a gel subjected to $N = 1$ extension, Eq. (3.20) yields $\Delta\lambda_1 = 2$ and Eq. (3.21) yields $\bar{\lambda}_1^{(1)} = 3$. During stress relaxation, the side length of the gel is

$$L_1^{(1)} = \bar{\lambda}_1^{(1)} L_o = L_1^{\max}. \tag{3.22}$$

For a gel subjected to $N = 2$ incremental planar or equibiaxial extensions, one has that $\Delta\lambda_1 = 1$ from Eq. (3.20). According to Eq. (3.21),

the gel is first stretched up to $\bar{\lambda}_1^{(1)} = 2$ from the swollen configuration $\mathcal{B}_o$ and then up $\bar{\lambda}_1^{(2)} = 3/2$. Therefore, the side lengths of the gel during stress relaxation are, respectively,

$$L_1^{(1)} = \bar{\lambda}_1^{(1)} L_o = 2L_o\,,$$
$$L_1^{(2)} = \bar{\lambda}_1^{(2)} L_1^{(1)} = \bar{\lambda}_1^{(2)}\bar{\lambda}_1^{(1)} L_o = L_1^{\max}\,. \tag{3.23}$$

For a gel subjected to $N = 4$ consecutive planar or equibiaxial extensions, $\Delta\lambda_1 = 1/2$ from Eq. (3.20). From Eq. (3.21), one has that the gel is stretched up to $\bar{\lambda}_1^{(1)} = 3/2$ from the swollen configuration $\mathcal{B}_o$ for the first time, $\bar{\lambda}_1^{(2)} = 4/3$ for the second time, $\bar{\lambda}_1^{(3)} = 5/4$ for the third time, and $\bar{\lambda}_1^{(4)} = 6/5$ for the fourth time. During the each of the kth stress relaxations, the side lengths of the gel are

$$\begin{aligned} L^{(1)} &= \bar{\lambda}_1^{(1)} L_p = (3/2)L_o,\\ L_1^{(2)} &= \bar{\lambda}_1^{(2)} L_1^{(1)} = \bar{\lambda}_1^{(2)}\bar{\lambda}_1^{(1)} L_o = 2L_o,\\ L_1^{(3)} &= \bar{\lambda}_1^{(3)} L_1^{(2)} = \bar{\lambda}_1^{(3)}\bar{\lambda}_1^{(2)}\bar{\lambda}_1^{(1)} L_o = (5/2)L_o,\\ L_1^{(4)} &= \bar{\lambda}_1^{(4)} L_1^{(3)} = \bar{\lambda}_1^{(4)}\bar{\lambda}_1^{(3)}\bar{\lambda}_1^{(2)}\bar{\lambda}_1^{(1)} L_o = 3L_o = L_1^{\max}. \end{aligned} \tag{3.24}$$

3.2. Fast and slow stresses

We assume that, at each kth extension, the gel is stretched up to $\bar{\lambda}_\alpha^{(k)}$ within a time interval $\Delta t < < t_d$, where t_d is the characteristic time of diffusion of the gel, and the stretches $\bar{\lambda}_\alpha^{(k)}$ are then held constant during a time interval $\Delta t > > t_d$ (Fig. 2). During such time interval, the thickness of the gel increases due to the water uptake and, consequently, the plane stresses decrease from their (fast) values, $\sigma_{f\alpha}^{(k)}$, to the (slow) values, $\sigma_\alpha^{(k)}$, with the difference between the fast and slow stress values representing the *diffusion-driven stress relaxation*. This stress relaxation is thus determined by the overall increase in volume of the gel. From Eqs. (2.3), (2.5), and (2.6), the non-zero axial components of the Cauchy stress, $\sigma_i = T_{ii}$ $(i = 1, 2, 3)$, can be found to be

$$\sigma_i = \frac{G}{J_d}\lambda_{di}^2 - p\,, \tag{3.25}$$

where λ_{di} are the non-zero components of the deformation gradient $\mathbf{F}_d$ and represent the stretches computed from the dry configuration $\mathcal{B}_d$. From the traction-free boundary condition at the top and bottom of the gel, $\sigma_3 = 0$, it follows that

$$p = \frac{G}{J_d}\lambda_{d3}^2 \quad \text{and} \quad \sigma_\alpha = \frac{G}{J_d}(\lambda_{d\alpha}^2 - \lambda_{d3}^2)\,. \tag{3.26}$$

The Eqs. $(3.26)_2$ can be used to compute both the fast stress, $\sigma_{f\alpha}^{(k)}$, and slow stress, $\sigma_\alpha^{(k)}$ using the different values of λ_{d3} and J_d. Indeed, the values of the applied axial stretches in the configuration immediately before the kth stress relaxation, the $\mathcal{B}_f^{(k)}$ configuration, and those during stress-relaxation, the $\mathcal{B}^{(k)}$ configuration, are both equal to

$$\lambda_{d\alpha}^{(k)} = \frac{L_\alpha^{(k)}}{L_d} = \bar{\lambda}_\alpha^{(k)}\bar{\lambda}_\alpha^{(k-1)}\cdots\lambda_p\lambda_o\,, \tag{3.27}$$

since the side lengths of the gel are kept constant during stress relaxation. On the contrary, the transverse stretch $\lambda_{d3}^{(k)}$ in the out-of plane direction changes during stress relaxation. The value $\lambda_{d3}^{(k)}$ at the end of the kth stress relaxation is determined by the chemical balance law given by Eqs. $(2.4)_1$ and $(3.26)_1$, as

$$\hat{\mu}(J_d^{(k)}) + \frac{1}{J_d^{(k)}}G(\lambda_{d3}^{(k)})^2\Omega = \mu_e \quad \text{with} \quad J_d^{(k)} = \lambda_{d1}^{(k)}\lambda_{d2}^{(k)}\lambda_{d3}^{(k)}\,, \tag{3.28}$$

where $\lambda_{d3}^{(0)} = \lambda_{p3}\lambda_o$. On the other hand, when the gel goes from the configuration $\mathcal{B}^{(k-1)}$ to the configuration $\mathcal{B}_f^{(k)}$, its volume does not change, that is $\bar{\lambda}_1^{(k)}\bar{\lambda}_2^{(k)}\lambda_{f3}^{(k)} = 1$. The transverse stretches, $\lambda_{f3}^{(k)}$ and $\lambda_{df3}^{(k)}$, are computed as follows (Fig. 2(b)):

$$\lambda_{f3}^{(k)} = \frac{1}{\bar{\lambda}_1^{(k)}\bar{\lambda}_2^{(k)}} \quad \text{and} \quad \lambda_{df3}^{(k)} = \frac{1}{\bar{\lambda}_1^{(k)}\bar{\lambda}_2^{(k)}}\lambda_{d3}^{(k-1)}\,. \tag{3.29}$$

Eq. $(3.26)_2$ with $\lambda_{d\alpha} = \lambda_{d\alpha}^{(k)}$ gives the fast stress $\sigma_{f\alpha}^{(k)}$ when $\lambda_{d3} = \lambda_{df3}^{(k)}$ and $J_d = \lambda_{d1}^{(k)}\lambda_{d2}^{(k)}\lambda_{df3}^{(k)}$ and the slow stress $\sigma_\alpha^{(k)}$ when $\lambda_{d3} = \lambda_{d3}^{(k)}$ and $J_d = \lambda_{d1}^{(k)}\lambda_{d2}^{(k)}\lambda_{d3}^{(k)}$.

3.3. The fast and slow stresses corresponding to one and two consecutive extensions

Consider the case in which the parallelepiped-shaped gel described above is subjected to N consecutive planar extensions. We want to evaluate explicitly the fast and slow stresses at each of these incremental extensions. We assume that the total maximum side length that the gel can achieve after the incremental extensions is $L_\alpha^{\max}$. For $N = 1$ extension up to $\bar{\lambda}_\alpha^{(1)}$, we obtain that the in-plane and the out-of-plane stretches immediately before stress relaxation are, respectively,

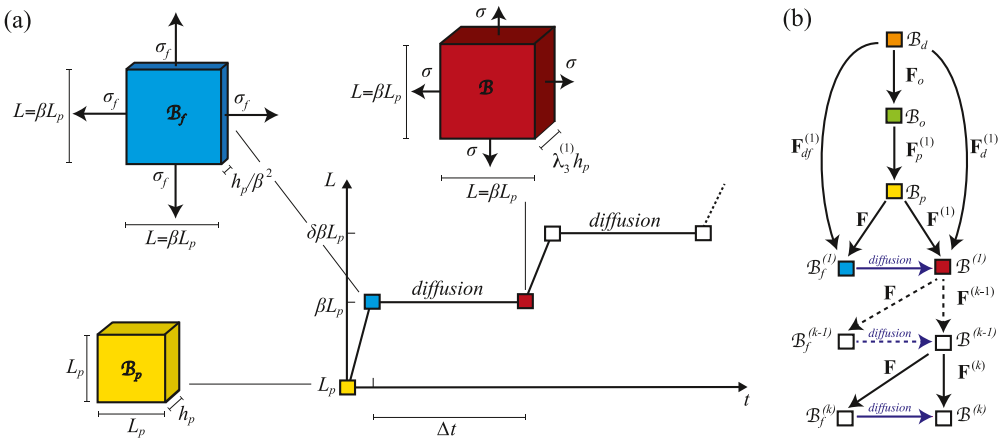

Fig. 2. (a) Schematic of the length L versus time t of a parallelepiped-shaped isotropic gel in various states: $\mathcal{B}_p$ is the pre-stretched state; $\mathcal{B}_f$ is the state immediately after the application of an equibiaxial stretch of magnitude $\beta = \bar{\lambda}_1^{(1)} = \bar{\lambda}_2^{(1)}$ (isochoric deformation) that generates a fast stress, σ_f; $\mathcal{B}$ is the steady swollen state attained under a constant equibiaxial stretch of magnitude β which leads to a slow stress, σ_f, over the time interval Δt. (b) Schematic of the various configurations and corresponding deformations used to evaluate the stress relaxation at incremental deformations. For $k = 1\cdots N$, $\mathcal{B}_f^{(k)}$ and $\mathcal{B}^{(k)}$ are the states where the fast stress and the slow stress are computed, respectively.

$$\lambda_{d\alpha}^{(1)} = \bar{\lambda}_{\alpha}^{(1)}\lambda_{p\alpha}\lambda_o \quad \text{and} \quad \lambda_{df3}^{(1)} = \frac{1}{\bar{\lambda}_1^{(1)}\bar{\lambda}_2^{(1)}}\lambda_{p3}\lambda_o\,, \tag{3.30}$$

and the change in volume is given by $J_d = J_p J_o$. By substituting $\lambda_{d\alpha} = \lambda_{d\alpha}^{(1)}$ and $\lambda_{d3} = \lambda_{df3}^{(1)}$ in Eq. (3.26)$_2$, the fast stresses $\sigma_{f\alpha}^{(1)}$ can be found to be

$$\sigma_{f\alpha}^{(1)} = \frac{G}{\lambda_o}\frac{1}{J_p}\left((\bar{\lambda}_{\alpha}^{(1)})^2\lambda_{p\alpha}^2 - \frac{\lambda_{p3}^2}{(\bar{\lambda}_1^{(1)})^2(\bar{\lambda}_2^{(1)})^2}\right). \tag{3.31}$$

At the end of the stress relaxation, the in-plane and the out-of-plane stretches are

$$\lambda_{d\alpha}^{(1)} = \bar{\lambda}_{\alpha}^{(1)}\lambda_{p\alpha}\lambda_o \quad \text{and} \quad \lambda_{d3}^{(1)} = \lambda_3^{(1)}\lambda_{p3}\lambda_o\,, \tag{3.32}$$

and the change in volume is $J_d = \lambda_3^{(1)}\bar{\lambda}_1^{(1)}\bar{\lambda}_2^{(1)}J_p J_o$.

By substituting $\lambda_{d\alpha} = \lambda_{d\alpha}^{(1)}$ and $\lambda_{d3} = \lambda_{d3}^{(1)}$ in Eq. (3.26)$_2$, the slow stresses $\sigma_{\alpha}^{(1)}$ can be found to be

$$\sigma_1^{(1)} = \frac{G}{\lambda_o}\left(\frac{\bar{\lambda}_1^{(1)}}{\bar{\lambda}_2^{(1)}}\frac{1}{\lambda_3^{(1)}}\frac{\lambda_{p1}}{\lambda_{p2}\lambda_{p3}} - \frac{\lambda_3^{(1)}}{\bar{\lambda}_1^{(1)}\bar{\lambda}_2^{(1)}}\frac{\lambda_{p3}}{\lambda_{p1}\lambda_{p2}}\right), \tag{3.33}$$

$$\sigma_2^{(1)} = \frac{G}{\lambda_o}\left(\frac{\bar{\lambda}_2^{(1)}}{\bar{\lambda}_1^{(1)}}\frac{1}{\lambda_3^{(1)}}\frac{\lambda_{p2}}{\lambda_{p1}\lambda_{p3}} - \frac{\lambda_3^{(1)}}{\bar{\lambda}_1^{(1)}\bar{\lambda}_2^{(1)}}\frac{\lambda_{p3}}{\lambda_{p1}\lambda_{p2}}\right). \tag{3.34}$$

The change in volume from the pre-stretched states $\mathcal{B}_p$ to the $\mathcal{B}^{(1)}$ state, $J_1 = \bar{\lambda}_1^{(1)}\bar{\lambda}_2^{(1)}\lambda_3^{(1)}$, depends on $\lambda_3^{(1)}$ and can be evaluated by solving the nonlinear Eq. (3.28). After noting that $J_d = J_1 J_p J_o$ and recalling that $J_o = \lambda_o^3$, $J_p = \lambda_{p1}\lambda_{p2}\lambda_{p3}$, $J_1 = \bar{\lambda}_1^{(1)}\bar{\lambda}_2^{(1)}\lambda_3^{(1)}$, this nonlinear equation can be written as

$$\hat{\mu}(J_1 J_p J_o) + \Omega\frac{G}{\lambda_o}\frac{J_1 J_p}{(\lambda_{p1}\bar{\lambda}_1^{(1)})^2(\lambda_{p2}\bar{\lambda}_2^{(1)})^2} = \mu_e\,. \tag{3.35}$$

For large deformations, $1/(J_1 J_p J_o) \to 0$ so that

$$\hat{\mu}(J_1 J_p J_o) \simeq \frac{RT}{\Omega}(\chi - 1/2)\frac{1}{J_1^2 J_p^2 J_o^2} \tag{3.36}$$

and

$$\frac{RT}{\Omega}(\chi - 1/2)\frac{1}{J_1^2 J_p^2 J_o^2} + \frac{G}{\lambda_o}\frac{J_1 J_p}{(\lambda_{p1}\bar{\lambda}_1^{(1)})^2(\lambda_{p2}\bar{\lambda}_2^{(1)})^2} = \frac{\mu_e}{\Omega}\,. \tag{3.37}$$

Now, by using Eq. (2.13), the above equation can be written as

$$\left(\frac{\mu_e}{\Omega} - \frac{G}{\lambda_o}\right)\frac{1}{J_1^2 J_p^2} + \frac{G}{\lambda_o}\frac{J_1 J_p}{(\lambda_{p1}\bar{\lambda}_1^{(1)})^2(\lambda_{p2}\bar{\lambda}_2^{(1)})^2} = \frac{\mu_e}{\Omega}\,. \tag{3.38}$$

We note that, for $\mu_e = 0$ and $\lambda_{p1} = \lambda_{p2} = \lambda_{p3} = 1$, that is, without pre-stretch, we get

$$J_1 = (\bar{\lambda}_1^{(1)}\bar{\lambda}_2^{(1)})^{2/3} \quad \text{and} \quad \lambda_3^{(1)} = (\bar{\lambda}_1^{(1)}\bar{\lambda}_2^{(1)})^{-1/3}\,. \tag{3.39}$$

Eq. (3.39)$_1$ corresponds to the Eq. (5) reported in Fujine et al. (2015); it expresses the fact that for planar extensions, that is, for $\bar{\lambda}_{\alpha}^{(1)} > 1$, the volume of the gel increases due to water absorption, and $J_1 > 1$.

On the other hand, initially $J_d = J_o$ and, hence, also $c_d = c_o$. Then, from Eqs. (2.4) and (2.9), the chemical potential μ of the water within the gel satisfies the following inequality

$$\mu = \hat{\mu}(c_o) + \Omega p_o\left(\frac{1}{\bar{\lambda}_1^{(1)}\bar{\lambda}_2^{(1)}}\right) < \hat{\mu}(c_o) + \Omega p_o\,, \tag{3.40}$$

for $\bar{\lambda}_{\alpha}^{(1)} > 1$, that is, under extension. Hence, the chemical potential within the body decreases instantaneously due to the extension. Consequently, the gel imbibes more water over time, the volume of the gel increases, and the generated stresses decrease.

For an equibiaxial extension starting from the stress-free swollen state $\mathcal{B}_o$ with no pre-stretch, we have $\lambda_{p1} = \lambda_{p2} = \lambda_{p3} = 1$ and we can set $\bar{\lambda}^{(1)} \equiv \bar{\lambda}_{\alpha}^{(1)}$. We can defined the amount of stress relaxation as $\Delta\sigma_{\alpha} = \sigma_{f\alpha}^{(1)} - \sigma_{\alpha}^{(1)}$ and, for an equibiaxial extension of an isotropic material, we can set $\Delta\sigma \equiv \Delta\sigma_{\alpha}$. It then follows that

$$\Delta\sigma = \frac{G}{\lambda_o}\left((\bar{\lambda}^{(1)})^2 - \frac{1}{(\bar{\lambda}^{(1)})^4}\right) - \frac{G}{\lambda_o}\left(\frac{1}{\lambda_3^{(1)}} - \frac{\lambda_3^{(1)}}{(\bar{\lambda}^{(1)})^2}\right). \tag{3.41}$$

We note that Eq. (3.41) can be used to evaluate stress relaxation, once the nonlinear Eq. (3.28) has been solved for $\lambda_3^{(1)}$; in our case, this is done numerically by using the built in algorithm 'FindRoot' in Mathematica (Wolfram Research, Inc., Mathematica, Version 11). Under the hypothesis of large deformations, and using Eq. (3.39)$_2$ with $\bar{\lambda}_{\alpha}^{(1)} = \bar{\lambda}^{(1)}$, Eq. (3.41) simplifies to

$$\Delta\sigma = \frac{G}{\lambda_o}((\bar{\lambda}^{(1)})^2 - (\bar{\lambda}^{(1)})^{-4} - (\bar{\lambda}^{(1)})^{2/3} + (\bar{\lambda}^{(1)})^{-8/3})\,. \tag{3.42}$$

We use Eq. (3.41) to evaluate the stress relaxation $\Delta\sigma$ under equibiaxial extension with $1 \le \bar{\lambda}_1^{(1)} = \bar{\lambda}_2^{(1)} \le 3$. We use similar equations to evaluate the stress relaxation for a planar extension with $1 \le \bar{\lambda}_1^{(1)} \le 3$ and $\bar{\lambda}_2^{(1)} = 1$, without pre-stretching ($\lambda_{p1} = \lambda_{p2} = \lambda_{p3} = 1$) and for an unequal planar extension with pre-stretches $L_{p1} = L_o$, $L_{p2} = (3/2)L_{p1}$ and $1 \le \bar{\lambda}_1^{(1)} = \bar{\lambda}_2^{(1)} \le 3$. In evaluating the stress relaxation, the values of the material parameters were selected to be those reported in Eqs. (2.10).

Fig. 3(a) shows the relative stress relaxation $\Delta\sigma_{\alpha}/\sigma_{f\alpha}^{(1)}$, versus L_1/L_o for a planar extension and an equibiaxial extension. The relative stress relaxation $\Delta\sigma_{\alpha}/\sigma_{f\alpha}^{(1)}$ for an unequal planar extension is presented in Fig. 3 (b).

The relative stress relaxation increases as the magnitude of the planar or equibiaxial extension ($\bar{\lambda}_1^{(1)} = L_1/L_o$) increases. This is in

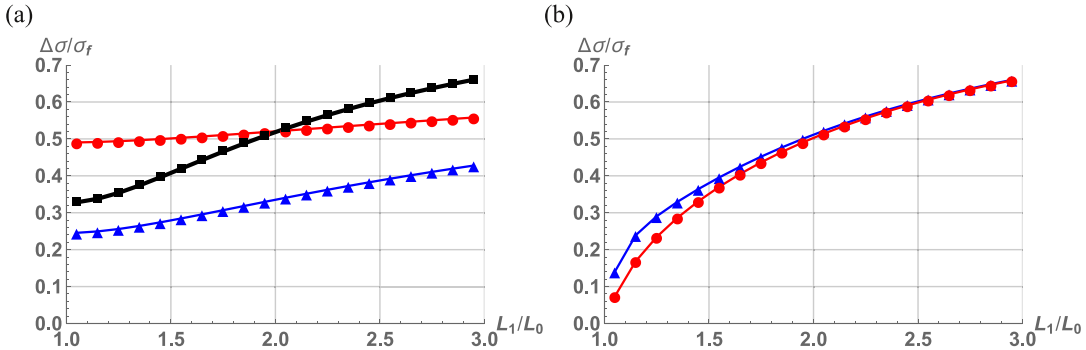

Fig. 3. (a) Relative stress relaxation curves, $\Delta\sigma_1/\sigma_{f1}^{(1)}$ (blue triangles) and $\Delta\sigma_2/\sigma_{f2}^{(1)}$ (red circles), versus L_1/L_0 for a planar extension with $\bar{\lambda}_2^{(1)} = 1$, and $\Delta\sigma_1/\sigma_{f1}^{(1)} = \Delta\sigma_2/\sigma_{f2}^{(1)}$ (black squares) versus L_1/L_0 for an equibiaxial extension with $\bar{\lambda}_1^{(1)} = \bar{\lambda}_2^{(1)}$. (b) Relative stress relaxation $\Delta\sigma_1/\sigma_{f1}^{(1)}$ (blue triangles) and $\Delta\sigma_2/\sigma_{f2}^{(1)}$ (red circles) versus L_1/L_0 for $\bar{\lambda}_2^{(1)} = 1$ and $L_{p2}/L_{p1} = 3/2$. (For interpretation of the references to colour in this figure legend, the reader is referred to the web version of this article.)

agreement with the experimental results reported in Fig. 7 in Fujine et al. (2015). For planar extension with $\bar{\lambda}_2^{(1)} = 1$, the relative stress relaxation increases differently in the two in-plane directions. On the contrary, for unequal biaxial extension, the relative stress relaxation is different and becomes equal in the two directions when the extension increases. This is due to the fact that the gel is first extended from the stress-free swollen state $\mathcal{B}_o$ to the pre-stretched state $\mathcal{B}_p$ such that $L_{p2}/L_{p1} = 3/2$ and then is further extended to the state $\mathcal{B}^{(1)}$ assuming that $\bar{\lambda}_2^{(1)}/\bar{\lambda}_1^{(1)} = 3/2$.

Next, we consider the fast and slow stresses that correspond to two (or more) consecutive extensions. For $N = 2$ consecutive extensions, we get that the in-plane stretch and the out-of-plane stretch immediately before stress relaxation are, respectively,

$$\lambda_{d\alpha}^{(2)} = \bar{\lambda}_\alpha^{(2)}\bar{\lambda}_\alpha^{(1)}\lambda_{p\alpha}\lambda_o \quad \text{and} \quad \lambda_{df3}^{(2)} = \frac{1}{\bar{\lambda}_1^{(2)}\bar{\lambda}_2^{(2)}}\lambda_3^{(1)}\lambda_{p3}\lambda_o\,, \tag{3.43}$$

and the change in volume is $J_d = J_1 J_p J_o$. By substituting $\lambda_{d\alpha} = \lambda_{d\alpha}^{(2)}$ and $\lambda_{d3} = \lambda_{df3}^{(2)}$ in Eqs. (3.26)$_2$, the fast stresses $\sigma_{f\alpha}^{(2)}$ can be found to be

$$\sigma_{f1}^{(2)} = \frac{G}{\lambda_o}\left(\frac{\bar{\lambda}_1^{(1)}}{\bar{\lambda}_2^{(1)}}\frac{\lambda_{p1}}{\lambda_{p2}\lambda_{p3}}\frac{(\bar{\lambda}_1^{(2)})^2}{\lambda_3^{(1)}} - \frac{\lambda_3^{(1)}}{\bar{\lambda}_1^{(1)}\bar{\lambda}_2^{(1)}(\bar{\lambda}_1^{(2)}\bar{\lambda}_2^{(2)})^2}\frac{\lambda_{p3}}{\lambda_{p1}\lambda_{p2}}\right), \tag{3.44}$$

$$\sigma_{f2}^{(2)} = \frac{G}{\lambda_o}\left(\frac{\bar{\lambda}_2^{(1)}}{\bar{\lambda}_1^{(1)}}\frac{(\bar{\lambda}_2^{(2)})^2}{\lambda_3^{(1)}}\frac{\lambda_{p2}}{\lambda_{p1}\lambda_{p3}} - \frac{\lambda_3^{(1)}}{\bar{\lambda}_1^{(1)}\bar{\lambda}_2^{(1)}(\bar{\lambda}_1^{(2)}\bar{\lambda}_2^{(2)})^2}\frac{\lambda_{p3}}{\lambda_{p1}\lambda_{p2}}\right). \tag{3.45}$$

At the end of the stress relaxation when the chemical equilibrium is achieved so that the gel is in the $\mathcal{B}^{(2)}$ state, the in-plane stretch and the out-of-plane stretch are, respectively,

$$\lambda_{d\alpha}^{(2)} = \bar{\lambda}_\alpha^{(1)}\lambda_{p\alpha}\lambda_o \quad \text{and} \quad \lambda_{d3}^{(2)} = \lambda_3^{(2)}\lambda_3^{(1)}\lambda_{p3}\lambda_o\,, \tag{3.46}$$

and the change in volume is $J_d = \lambda_3^{(2)}\bar{\lambda}_1^{(2)}\bar{\lambda}_2^{(2)}\lambda_3^{(1)}\bar{\lambda}_1^{(1)}\bar{\lambda}_2^{(1)}J_pJ_o$. Substituting $\lambda_{d\alpha} = \lambda_{d\alpha}^{(2)}$ and $\lambda_{d3} = \lambda_{d3}^{(2)}$ into Eq. (3.26)$_2$ gives the following slow stresses $\sigma_\alpha^{(1)}$:

$$\sigma_1^{(2)} = \frac{G}{\lambda_o}\left(\frac{\bar{\lambda}_1^{(2)}\bar{\lambda}_1^{(1)}}{\bar{\lambda}_2^{(2)}\bar{\lambda}_2^{(1)}}\frac{1}{\lambda_3^{(2)}\lambda_3^{(1)}}\frac{\lambda_{p1}}{\lambda_{p2}\lambda_{p3}} - \frac{\lambda_3^{(2)}\lambda_3^{(1)}}{\bar{\lambda}_1^{(2)}\bar{\lambda}_2^{(2)}\bar{\lambda}_1^{(1)}\bar{\lambda}_2^{(1)}}\frac{\lambda_{p3}}{\lambda_{p1}\lambda_{p2}}\right), \tag{3.47}$$

$$\sigma_2^{(2)} = \frac{G}{\lambda_o}\left(\frac{\bar{\lambda}_2^{(2)}\bar{\lambda}_2^{(1)}}{\bar{\lambda}_1^{(2)}\bar{\lambda}_1^{(1)}}\frac{1}{\lambda_3^{(2)}\lambda_3^{(1)}}\frac{\lambda_{p2}}{\lambda_{p1}\lambda_{p3}} - \frac{\lambda_3^{(2)}\lambda_3^{(1)}}{\bar{\lambda}_1^{(2)}\bar{\lambda}_2^{(2)}\bar{\lambda}_1^{(1)}\bar{\lambda}_2^{(1)}}\frac{\lambda_{p3}}{\lambda_{p1}\lambda_{p2}}\right). \tag{3.48}$$

We note that the fast and slow stresses that result from more than two extensions ($N > 2$) can be obtained easily following a similar procedure as the one used here for two consecutive extensions.

3.4. The history-dependent fast stress response

Let us discuss some results of our analysis which show how incremental biaxial extensions affect stress relaxation and, consequently, could affect the design of hydrogel-based actuators. Firstly, we observe that, as expected, if the gel is not subjected to any extension from the state $\mathcal{B}^{(k-1)}$ to the state $\mathcal{B}^{(k)}$, the slow stress $\sigma_\alpha^{(k-1)}$ is equal to the fast stress $\sigma_{f\alpha}^{(k)}$. Indeed, for $N = 2$, Eqs. (3.44) at $\bar{\lambda}_1^{(2)} = \bar{\lambda}_2^{(2)} = 1$ are equal to Eqs. (3.33):

$$\sigma_{f\alpha}^{(2)} = \sigma_\alpha^{(1)} \quad \text{at} \quad \bar{\lambda}_\alpha^{(2)} = 1\,. \tag{3.49}$$

Secondly, it is well known that the slow stress does not depend on the history of deformation. In other words, if the initial side lengths $L_{p\alpha}$ of the gel increase to the final side lengths $L_\alpha^{\max}$ through the extension $\bar{\lambda}_\alpha^{(1)} = L_\alpha^{\max}/L_{p\alpha}$ or through the extension $\bar{\lambda}_\alpha^{(2)}\bar{\lambda}_\alpha^{(1)} = L_\alpha^{\max}/L_{p\alpha}$ that occurs in $N = 2$ steps, then the same slow stress is obtained. To show this, let us assume for simplicity that $L_{p\alpha} = L_o$ so that the gel is not pre-stretched but it is extended starting from the stress-free swollen state $\mathcal{B}_o$. Then, the slow stress that corresponds to the first and second extensions are

$$\sigma_\alpha^{(1)} = \frac{G}{\lambda_o}\left(\frac{L_1^{\max}}{L_2^{\max}}\frac{1}{\lambda_3^{(1)}} - \frac{L_o^2}{L_1^{\max}L_2^{\max}}\lambda_3^{(1)}\right), \tag{3.50}$$

and

$$\sigma_\alpha^{(2)} = \frac{G}{\lambda_o}\left(\frac{L_1^{\max}}{L_2^{\max}}\frac{1}{\lambda_3^{(1)}\lambda_3^{(2)}} - \frac{L_o^2}{L_1^{\max}L_2^{\max}}\lambda_3^{(1)}\lambda_3^{(2)}\right), \tag{3.51}$$

respectively. The transverse stretch $\lambda_3^{(1)}$ in Eq. (3.50) can be computed by solving the nonlinear Eq. (3.35) by substituting

$$\lambda_{d3} = \lambda_{d3}^{(2)} = \lambda_3^{(1)}\lambda_o \quad \text{and} \quad J_d = J_d^{(1)} = \lambda_3^{(1)}\frac{L_1^{\max}L_2^{\max}}{L_o^2}J_o\,. \tag{3.52}$$

Similarly, the transverse stretch $\lambda_3^{(1)}\lambda_3^{(2)}$ in Eq. (3.51) can be computed by solving the nonlinear Eq. (3.35) with

$$\lambda_{d3} = \lambda_{d3}^{(2)} = \lambda_3^{(2)}\lambda_3^{(1)}\lambda_o \quad \text{and} \quad J_d = J_d^{(2)} = \lambda_3^{(2)}\lambda_3^{(1)}\frac{L_1^{\max}L_2^{\max}}{L_o^2}J_o\,. \tag{3.53}$$

Because the solutions of the nonlinear Eq. (3.35) with unknown $\lambda_3^{(1)}$ or $\lambda_3^{(1)}\lambda_3^{(2)}$ are equal, the associated slow stresses (3.50) and (3.51) computed from $\lambda_3^{(1)}$ or $\lambda_3^{(1)}\lambda_3^{(2)}$, respectively, are also equal.

On the contrary, the fast stress does depend on the history of deformation. This is an interesting finding that, to the best of our knowledge, has never been noted explicitely. In order to demonstrate such dependency, let us assume again that the gel is extended from the stress-free swollen state with no pre-stretch. Then, the parallelepiped-shaped gel of initial side lengths L_o can be stretched so that the final side lengths are $L_\alpha^{\max}$ either through a single extension that is defined by $\bar{\lambda}_\alpha^{(1)}$ or through two (or more) extensions that are defined by $\bar{\lambda}_\alpha^{(2)}\bar{\lambda}_\alpha^{(1)}$. The fast stress is lower when the side lengths are increased to $L_\alpha^{\max}$ through two (or more) extensions. This is due to the increase in volume that is caused by the uptake of solvent that occurs during the first extension, and it can be easily verified using Eqs. (3.31) and (3.44). By replacing $\bar{\lambda}_\alpha^{(1)}$ with $L_\alpha^{\max}/L_o$ in Eq. (3.31), we obtain the fast stress that corresponds to $N = 1$ extension and, by replacing $\bar{\lambda}_\alpha^{(1)}\bar{\lambda}_\alpha^{(2)}$ with $L_\alpha^{\max}/L_o$ in Eq. (3.44), we obtain the fast stress that corresponds to $N = 2$ consecutive extensions. It follows that

$$\sigma_{f\alpha}^{(1)} - \sigma_{f\alpha}^{(2)} = \frac{G}{\lambda_o}\left(\frac{(L_\alpha^{\max})^2}{L_o^2}\left(1 - \frac{1}{J_1}\right) + \frac{L_o^4}{(L_1^{\max})^2(L_\alpha^{\max})^2}(J_1 - 1)\right).$$

Since $J_1 > 1$, then

$$\sigma_{f\alpha}^{(1)} - \sigma_{f\alpha}^{(2)} > 0\,, \tag{3.54}$$

that is, the fast stress that corresponds to $N = 1$ extension is higher than the fast stress that corresponds to the $N = 2$ consecutive extensions that lead to an equal side length $L_\alpha^{\max}$ of the gel. Because the fast stress depends on the history of deformation, the stress relaxation that is computed from such stress also depends on the history of deformation as discussed below for the case of a planar extension and the case of an equibiaxial extension.

4. Stress-relaxation due to incremental extensions

We investigate the dependence of stress relaxation on the history of deformation by considering a planar extension and an equi-biaxial extension that occur in one or a few steps. Fig. 4 shows the diffusion-driven history dependence of the stress response for a planar extension assuming that the gel is stretched from the stress-free swollen configuration $\mathcal{B}_o$ with no pre-stretching ($\lambda_{p1} = \lambda_{p2} = \lambda_{p3} = 1$) in $N = 1$, $N = 2$, and $N = 4$ steps. Specifically, we consider the case in which the side length L_1 of the gel increases from L_o to $L_1^{\max} = 3L_o$ and the side length L_2 does not change ($L_2 = L_o$).

First, we consider the case in which the gel is stretched up to $\bar{\lambda}_1^{(1)} = 3$ with $\bar{\lambda}_2^{(1)} = 1$ in $N = 1$ step. Thus, from Eq. (3.20), it follows that $\Delta\lambda_1 = 3$. The dimensionless fast and slow stresses, $\sigma_{f\alpha}^{(1)}/G$ and σ_α/G

($\alpha = 1, 2$), for the stretch interval $1 \le L_1/L_o \le 3$ are represented in Fig. 4(a)–(b). The difference between these two quantities provides the dimensionless stress relaxation for any value of L_1/L_o.

Secondly, we assume that the gel is extended so that the final length $L_1^{\max} = 3L_o$ is achieved in $N = 2$ consecutive planar extensions so that L_1/L_0 increases from 1 to 2 and from 2 to 3 (Fig. 4(c)–(d)). From Eq. (3.20), it follows that $\Delta\lambda_1 = 1$ with $\Delta\lambda_2 = 0$. According to Eqs. (3.23), the side length of the gel along the direction $\mathbf{e}_1$ increases firstly from L_o to $L_1^{(1)} = 2L_o$ and then from $L_1^{(1)}$ to $L_1^{(2)} = (3/2)L_1^{(1)} = 3L_o$. The dimensionless fast and slow stresses, $\sigma_{f\alpha}^{(1)}/G$ and $\sigma_{\alpha}^{(1)}/G$, at the first extension $\bar{\lambda}_1^{(1)} = 2$ are presented in Fig. 4(c)–(d). The side length of the gel is then further stretched of $\bar{\lambda}_1^{(2)} = 3/2$ so that $\bar{\lambda}_1^{(2)}\bar{\lambda}_1^{(1)} = 3$. The fast dimensionless stress at the final side length $L_1^{(2)} = L_1^{\max} = 3L_o$ achieved after the two consecutive extensions $\bar{\lambda}_1^{(1)} = 2$ and $\bar{\lambda}_1^{(2)} = 3/2$ is much lower than the one attained when the gel reaches the same final side length $L_1^{\max}$ in just one extension.

Finally, we consider the case in which the gel reaches the final side length $L_1^{\max} = 3L_0$ in $N = 4$ consecutive planar extensions (Fig. 4(e)–(f)). In this case, Eq. (3.20) leads to $\Delta\lambda_1 = 1/2$ with $\Delta\lambda_2 = 0$ and, from Eqs. (3.24), the side length of the gel is firstly increased from L_o to $L_1^{(1)}$ and then to $L_1^{(2)}$, $L_1^{(3)}$, and $L_1^{(4)} = 3L_o$. The dimensionless fast and slow stresses up to $\bar{\lambda}_1^{(1)} = 3/2$, from $\bar{\lambda}_1^{(1)}$ to $\bar{\lambda}_1^{(2)} = 4/3$ corresponding to $\bar{\lambda}_1^{(2)}\bar{\lambda}_1^{(1)} = 2$, from $\bar{\lambda}_1^{(2)} = 4/3$ to $\bar{\lambda}_1^{(3)} = 5/4$ corresponding to $\bar{\lambda}_1^{(3)}\bar{\lambda}_1^{(2)}\bar{\lambda}_1^{(1)} = 5/2$, and from $\bar{\lambda}_1^{(3)} = 5/4$ to $\bar{\lambda}_1^{(4)} = 6/5$ corresponding to $\bar{\lambda}_1^{(4)}\bar{\lambda}_1^{(3)}\bar{\lambda}_1^{(2)}\bar{\lambda}_1^{(1)} = 3$ are reported in Fig. 4(e)-(f). Again, the dimensionless stress relaxation at each of the stretches can be computed by calculating the differences between the slow and fast dimensionless stresses as shown in Fig. 5.

As expected, the stresses are much higher in the direction in which the gel is stretched (Fig. 4(a),(c) and (e)) although the overall stress relaxation is higher in the direction that is kept fixed (Fig. 4(b),(c) and (d)). Moreover, the stress relaxation is reduced by increasing the number of steps that are used to achieve a given extension of the gel. In particular, for an extension that occurs in $N = 4$ consecutive extensions, the dimensionless stress relaxation is also presented in Fig. 5 at different extensions.

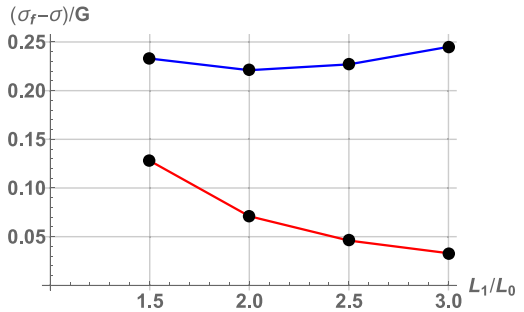

Fig. 5. Dimensionless stress relaxation computed as $(\sigma_{f1} - \sigma_1)/G$ (blue line) and $(\sigma_{f2} - \sigma_2)/G$ (red line) corresponding to the planar extension shown in Fig. 4(e)–(f). (For interpretation of the references to colour in this figure legend, the reader is referred to the web version of this article.)

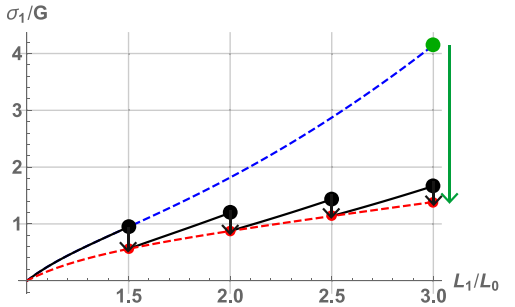

Fig. 6. Fast (dashed blue line) and slow (dashed red line) dimensionless stress for an equibiaxial extension for $1 \le L_1/L_0 \le 3$ with $L_2 = L_1$. The green circle represents the fast stress achieved in $N = 1$ step. The black circles represent the fast stress achieved in 4 steps, with L_1/L_0 that goes from 1 to 1.5, 1.5 to 2, 2 to 2.5, and 2.5 to 3. Arrows between the green or black circles and the red circles identify the dimensionless stress relaxation. Note that $\sigma_2/G = \sigma_1/G$. (For interpretation of the references to colour in this figure legend, the reader is referred to the web version of this article.)

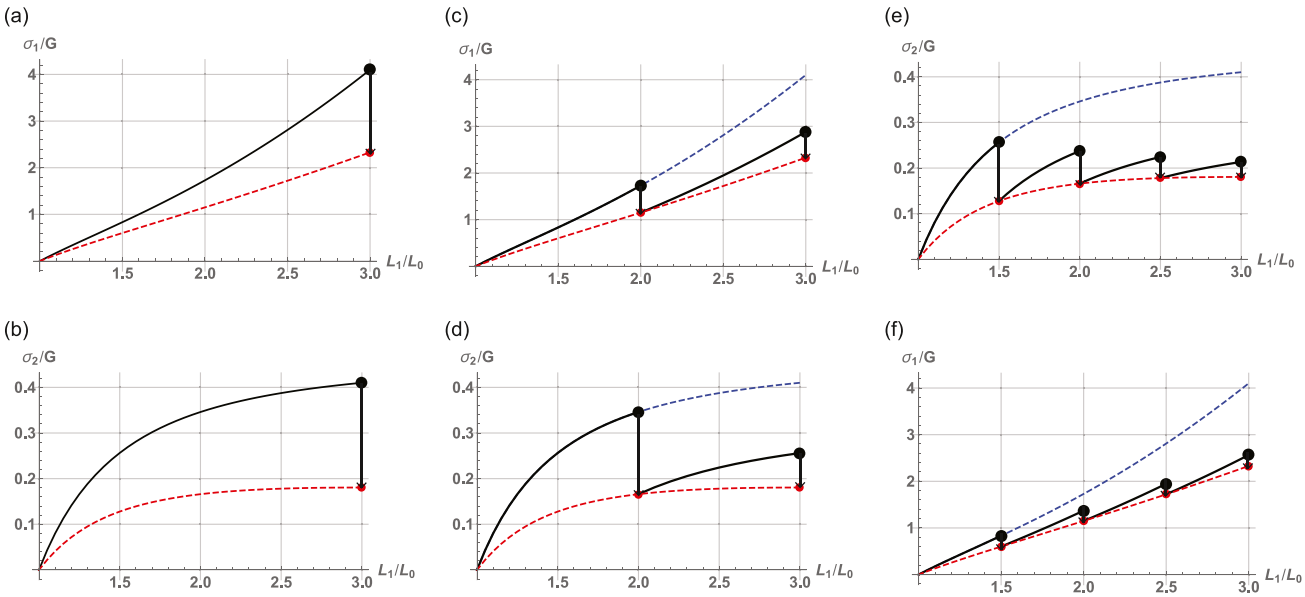

Fig. 4. Fast (black solid line) and slow (red dashed line) dimensionless stresses in three different planar extensions for $1 \le L_1/L_0 \le 3$ with $L_2 = L_0$. Black circles and red circles represent the fast and slow stresses, respectively, obtained in (a)–(b) $N = 1$ step with L_1/L_0 that goes from 1 to 3, (c)–(d) $N = 2$ steps with L_1/L_0 that goes from 1 to 2 and from 2 to 3. (e)–(f) $N = 4$ steps with L_1/L_0 that goes from 1 to 1.5, 1.5 to 2, 2 to 2.5, and 2.5 to 3. Arrows between the black and red circles identify the dimensionless stress relaxation. Dashed blue line represents dimensionless fast stress for a single extension up to $L_1/L_0 = 3$. (For interpretation of the references to colour in this figure legend, the reader is referred to the web version of this article.)

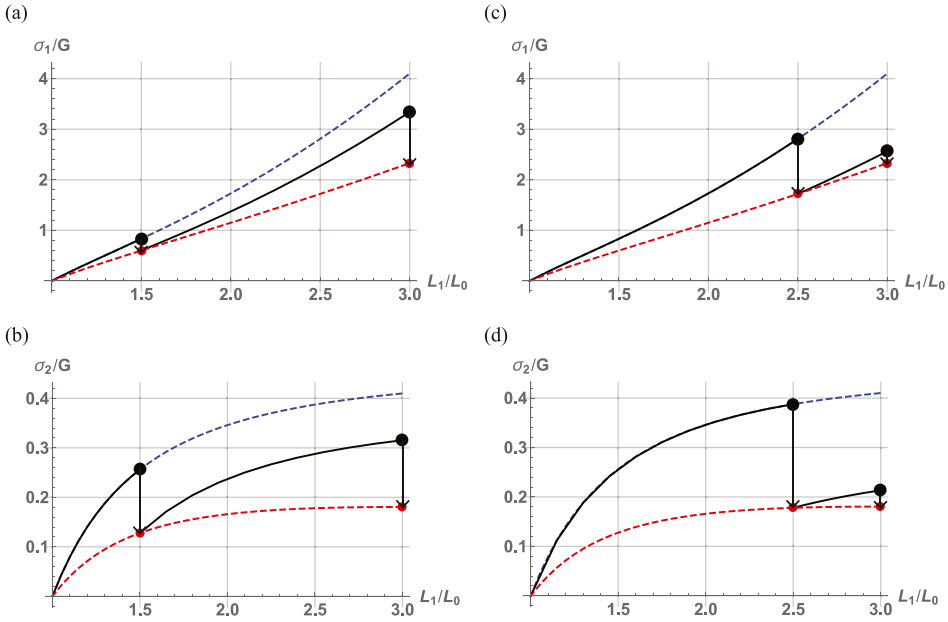

Fig. 7. Fast (black solid line) and slow (red dashed line) dimensionless stresses in two different planar extensions for $1 \le L_1/L_o \le 3$ with $L_2 = L_0$. Black circles and red circles represent the fast and slow stresses, respectively, obtained in $N = 2$ steps so that L_1/L_o goes up to (a)-(b) first $L_1/L_o = 1.5$ and then $L_1/L_o = 3$ and (c)-(d) first $L_1/L_o = 2.5$ and then $L_1/L_o = 3$. Arrows between the black and red circles identify the dimensionless stress relaxation. Dashed blue line represents dimensionless fast stress for a single extension up to $L_1/L_0 = 3$. (For interpretation of the references to colour in this figure legend, the reader is referred to the web version of this article.)

Similarly, one can compute the dimensionless fast and slow stresses that result from an equibiaxial extension in $N = 1$ step or $N = 4$ steps and the dimensionless stress relaxation (Fig. 6).

4.1. Effect of extension magnitude

The magnitude of the extension also influences the amount of stress relaxation. We investigate this effect by considering a planar extension in $N = 2$ consecutive steps of a gel that is in stress-free swollen configuration $\mathcal{B}_o$. The final length $L_1^{\max} = 3L_o$ of the gel is attained via two consecutive extensions of different magnitude. First, the side length of the gel is increased from L_o to $L_1^{(1)} = (3/2)L_o$ and then from $L_1^{(1)}$ to $L_1^{(2)} = 2L_1^{(1)} = 3L_o$ (Fig. 7(a)). Second, the side length is increased from L_o to $L_1^{(1)} = (5/2)L_o$, and then from $L_1^{(1)}$ to $L_1^{(2)} = (6/5)L_1^{(1)} = 3L_o$ (Fig. 7(b)). In Fig. 7, the slow and fast dimensionless stress responses σ_α and $\sigma_{f\alpha}$ are reported. One can observed that changing the magnitude of the intermediate extensions changes the final dimensionless stress relaxation.

4.2. Volume change

Figs. 4 and 5 show that the fast stress and the stress relaxation strongly depend on the deformation history of the gel. This characteristic behavior is determined by the water uptake and subsequent change in volume that occurs when the gel is stretched. We compute the water uptake (or, equivalently, change in volume) for a single planar or equibiaxial extension and for incremental equibiaxial extensions.

Firstly, we consider the usual parallelepiped-shaped gel with side of lengths L_o and thickness h_o in the stress-free swollen state $\mathcal{B}_o$. Starting from this configuration, the gel undergoes a single planar extension so that $L_1^{(1)} = 3L_o$ whereas $L_2^{(1)} = L_o$ and a single equibiaxial extension so that $L_1^{(1)} = L_2^{(1)} = 3L_o$ ($N = 1$). The change in volume given by J_d/J_o is reported in Fig. 8(a). As expected, the change in volume that occurs during an equibiaxial extension is higher than the one that occurs during a planar extension.

Secondly, we consider the case of a gel subjected to $N = 4$ consecutive planar extensions and $N = 4$ consecutive equibiaxial extensions again from the stress-free swollen state $\mathcal{B}_o$ and such that the final side lengths of the gel are $L_1^{(1)} = 3L_o$ and $L_2^{(1)} = L_o$ for planar extension and $L_1^{(1)} = L_2^{(1)} = 3L_o$ for equibiaxial extension. At the kth extension, the change in volume before diffusion starts, when the gel is in the $\mathcal{B}_f^{(k)}$ state can be computed as $J_f^{(k)}/J_o$. We note that since the extension after the $(k-1)$th stress relaxation from the $\mathcal{B}^{(k-1)}$ state to the $\mathcal{B}_f^{(k)}$ state is isochoric, $J^{(k-1)} = J_f^{(k)}$ so $J_f^{(k)}$ is determined by the change in volume $J^{(k-1)}$ that occurs at the $(k-1)$th extension. Fig. 8 (b) presents $(J_d - J_f)/J_o$ at each of the four incremental planar and equibiaxial extensions. One can note that this quantity decreases as the number of extension increases in planar tests whereas is almost constant in equibiaxal tests.

5. Conclusions

We presented an investigation of the history dependence of the diffusion-driven stress response of gels subjected to planar incremental extensions. The stress reduction at each incremental extension was computed as the difference between the stress before diffusion starts and the stress at the steady-state diffusion. The stress relaxation was found to greatly depend on both the number and magnitude of incremental extensions that lead to a given extension. To the best of our knowledge, these theoretical findings have never been presented. The proposed modeling framework could guide the development of control strategies of hydrogel-based actuators that need to attain a prescribed deformation in multiple steps.

Competing

No competing interests.

Acknowledgments

R.D. and P.N. acknowledge financial support from La Sapienza University through Mobility Grant for International Agreements (D.R.

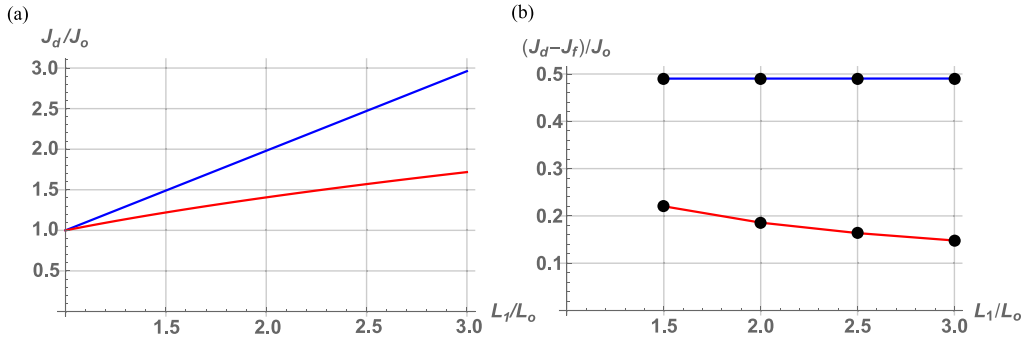

Fig. 8. (a) Volume change, J_d/J_o, occurring during a planar extension (red line) and an equibiaxial extension (blue line). (b) Difference $(J_d - J_f)/J_o$ in volume changes occurring at four consecutive planar extensions (red line) and equibiaxial extensions (blue line). (For interpretation of the references to colour in this figure legend, the reader is referred to the web version of this article.)

1729/2017). R.D. also acknowledges financial support from NSF Grant No. 1804432.

References

Bertrand, T., Peixinho, J., Mukhopadhyay, S., Minn, C.W.M., 2016. Dynamics of swelling and drying in a spherical gel. Phys. Rev. Appl. 6, 064010. https://doi.org/10.1103/PhysRevApplied.6.064010. http://link.aps.org/doi/10.1103/PhysRevApplied.6.064010

Curatolo, M., Nardinocchi, P., Puntel, E., Teresi, L., 2017. Transient instabilities in the swelling dynamics of a hydrogel sphere. J. Appl. Phys. 122 (14), 145109. https://doi.org/10.1063/1.5007229.

Flory, P.J., Rehner, J., 1943a. Statistical mechanics of cross-linked polymer networks i. Rubberlike elasticity. J. Chem. Phys. 11 (11), 512–520.

Flory, P.J., Rehner, J., 1943b. Statistical mechanics of cross-linked polymer networks ii. Swelling. J. Chem. Phys. 11 (11), 521–526.

Fujine, M., Takigawa, T., Urayama, K., 2015. Strain-driven swelling and accompanying stress reduction in polymer gels under biaxial stretching. Macromolecules 48 (11), 3622–3628. https://doi.org/10.1021/acs.macromol.5b00642.

Hong, W., Liu, Z., Suo, Z., 2009. Inhomogeneous swelling of a gel in equilibrium with a solvent and mechanical load. Int. J. Solids Struct. 46 (17), 3282–3289. https://doi.org/10.1016/j.ijsolstr.2009.04.022. http://www.sciencedirect.com/science/article/pii/S0020768309001899

Lucantonio, A., Nardinocchi, P., Teresi, L., 2013. Transient analysis of swelling-induced large deformations in polymer gels. J. Mech. Phys. Solids 61 (1), 205–218. https://doi.org/10.1016/j.jmps.2012.07.010. http://www.sciencedirect.com/science/article/pii/S0022509612001548

Nardinocchi, P., Pezzulla, M., Teresi, L., 2015a. Steady and transient analysis of anisotropic swelling in fibered gels. J. Appl. Phys. 118 (24). https://doi.org/10.1063/1.4938737.

Nardinocchi, P., Pezzulla, M., Teresi, L., 2015b. Anisotropic swelling of thin gel sheets. Soft Matter 11, 1492–1499. https://doi.org/10.1039/C4SM02485K.

Nardinocchi, P., Teresi, L., 2016. Actuation performances of anisotropic gels. J. Appl. Phys. 120 (21), 215107. https://doi.org/10.1063/1.4969046.

Pence, T. J.,. On the formulation of boundary value problems with the incompressible constituents constraint in finite deformation poroelasticity. Math. Methods Appl. Sci. 35 (15), 1756–1783. https://onlinelibrary.wiley.com/doi/abs/10.1002/mma.2541. 10.1002/mma.2541.

Selvadurai, A., Suvorov, A., 2017. On the inflation of poro-hyperelastic annuli. J. Mech. Phys. Solids 107, 229–252. https://doi.org/10.1016/j.jmps.2017.06.007. http://www.sciencedirect.com/science/article/pii/S0022509617302958

Takigawa, T., Urayama, K., Morino, Y., Masuda, T., 1993. Simultaneous swelling and stress relaxation behavior of uniaxially stretched polymer gels. Polym. J. 25, 929–937. https://www.nature.com/articles/pj1993114#references

Urayama, K., Takigawa, T., 2012. Volume of polymer gels coupled to deformation. Soft Matter 8, 8017–8029. https://doi.org/10.1039/C2SM25359C.

Urayama, K., Takigawa, T., Masuda, T., 1994. Stress relaxation and creep of polymer gels in solvent under uniaxial and biaxiai deformations. Rheol. Acta 33, 89–98. https://link.springer.com/content/pdf/10.1007/BF00366753.pdf

Wineman, A., Rajagopal, K., 1992. Shear induced redistribution of fluid within a uniformly swollen nonlinear elastic cylinder. Int. J. Eng. Sci. 30 (11), 1583–1595. https://doi.org/10.1016/0020-7225(92)90127-3. http://www.sciencedirect.com/science/article/pii/0020722592901273

Yohsuke, B., Urayama, K., Takigawa, T., Ito, K., 2011. Biaxial strain testing of extremely soft polymer gels. Soft Matter 7, 2632–2638. https://doi.org/10.1039/C0SM00955E.